

Sound Speed Estimation for Underground Acoustical Imaging -A Study on Array Arrangement-

地中映像化における音速推定に関する研究 -アレイ設置に関する検討-

Dai Chimura[‡], Kengo Izumida, Ryo Toh, and Seichi Motooka (Facult. Eng., Chiba Inst. Tech.)

千村 大[‡], 泉田 健吾, 陶 良, 本岡 誠一 (千葉工大・工)

1. Introduction

Acoustical imaging is efficient for nondestructively detecting underground objects such as pipelines and buried relics. We have proposed an ultrasonic underground imaging method using an electromagnetic-induction (EMI) type sound source and an amplitude correlation synthesis processing (ACSP) method^{1,2)}. By using the EMI type sound source, an impulsive ultrasonic with higher energy is emitted in underground, and, the ACSP method derives an imaging with a higher SNR.

Moreover, the array arrangements have been studied for the higher resolution imaging^{3,4)}. We have discussed two types of array arrangement: a cross-type arrangement and a circular-type arrangement. The cross-type receivers are arranged as two cross lines and the circular-type receivers are arranged in a circle. The imaging result using the circular-type arrangement reduced false images comparing with that using the cross-type arrangement.

On the other hand, Because of uncertain underground circumstances such as medium and moisture content, a sound speed for the imaging is uncertain. For higher accuracy imaging, sound speed estimation is expected.

Here, we propose sound speed estimation for underground imaging by comparing the maximum imaging value. If we use the correct sound speed, time delay processing correctly agrees with surveyed point, and the imaging result will have a higher value than that using an incorrect sound speed.

This paper discusses the effectiveness of array arrangement on sound estimation for underground imaging by simulation.

2. Imaging Method

2.1. Array Arrangement

The cross-type and the circular-type arrangements are shown in Figs. 1 and 2. The EMI type sound source and 12 receivers R_{ij} ($i = 1, 2, 3, 4$; $j = 1, 2, 3$) are arranged on the x - y plane, and z -axis denotes the depth direction of underground.

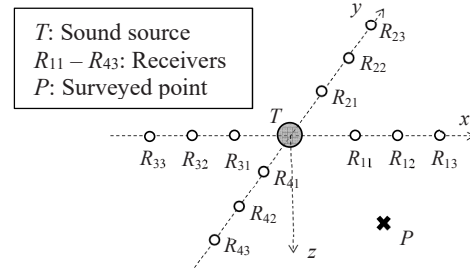


Fig. 1 Cross-type arrangement.

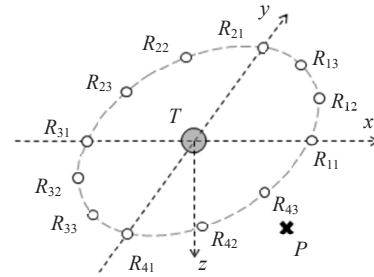


Fig. 2 Circular-type arrangement

2.2. Amplitude Correlation Synthesis Processing method

The imaging value H_P of a surveyed point $P(x, y, z)$ is calculated from the amplitudes of the signals obtained by each receivers. The amplitude A_{Pij} is calculated from the received signal $S_{ij}(t)$ as follows:

$$A_{Pij} = S_{ij} \left(\frac{l_{P0} + l_{Pij}}{c} \right), \quad (1)$$

where l_{P0} , l_{Pij} , and c are a range from sound source to $P(x, y, z)$, a range from $P(x, y, z)$ to the R_{ij} , and sound speed, respectively.

The imaging value H_P is calculated from A_{Pij} as follows:

$$H_P = \left| \sum_{\alpha, \beta, \zeta, \eta=1,2,3} CM(A_{P1\alpha}, A_{P2\beta}, A_{P3\zeta}, A_{P4\eta}) \right|. \quad (2)$$

Here, $CM(\cdot)$ is conditional multiplication function as follows:

$$CM(A_{P1\alpha}, A_{P2\beta}, A_{P3\zeta}, A_{P4\eta}) = \begin{cases} \text{sgn}(A_{P1\alpha}) \cdot A_{P1\alpha} \cdot A_{P2\beta} \cdot A_{P3\zeta} \cdot A_{P4\eta} & \text{all polarities are same} \\ 0, & \text{others} \end{cases} \quad (3)$$

3. Sound Speed Estimation Method

The sound speed is estimated from the maximum of the imaging value. The correct sound speed derives the higher imaging value when the object is located on the surveyed point. The estimated sound speed \hat{c} is shown as follows:

$$\hat{c} = \arg \max_c H_p(c), \quad (4)$$

where $H_p(c)$ is the imaging value corresponding to the sound speed.

4. Simulation Condition

4.1. Transmitting Signal and Received Signal

The transmitting signal is assumed to be launched by the EMI sound source. The transmitting impulsive signal $S_0(t)$ is assumed as follows:

$$S_0(t) = \exp(-2f_a t) \cdot \sin(2\pi f_m t). \quad (5)$$

Here, f_a and f_m are a main driving frequency (400 [Hz]) and a received signal frequency (300 [Hz]), respectively.

The received signal $S_{ij}(t)$ is calculated by simulation arrangement as follows:

$$S_{ij}(t) = \frac{1}{(l_{M0} + l_{Mij})^2} S_0\left(t - \frac{l_{M0} + l_{Mij}}{c_0}\right). \quad (6)$$

Here, l_{M0} , l_{Mij} , and c_0 are a range from sound source to the object, a range from the object to the receivers, and a simulated sound speed (190 [m/s]), respectively.

4.2. Simulation Arrangement

The cross-type arrangement locates the receivers with $x = -1.2, -0.8, -0.4, 0.4, 0.8, 1.2$ [m] on x -axis and $y = -1.2, -0.8, -0.4, 0.4, 0.8, 1.2$ [m] on y -axis. The circular-type arrangement locates the receivers with 0.8 [m] diameter. The object is placed at a location (0.6, 0.0, 1.2).

5. Results and discussion

The examples of the calculated image are shown in Fig. 3. The images calculated from the correct sound speed show the object with the correct location (shown as \times).

The sound speed estimation is shown in Fig. 4. The sound speed estimation with the cross-type arrangement shows the highest imaging value when the correct sound speed is employed. When the incorrect sound speed is employed for imaging calculation, the imaging value is lower because of the phase aberration on time delay processing.

However, the sound speed estimation with the circular-type arrangement shows almost identical imaging values even if the incorrect sound speed is employed. We suppose that the main reason is a depth of focus. When the array arrangement has the deep focus depth, a distinct focus is obtained even if the incorrect sound speed is employed, and the image

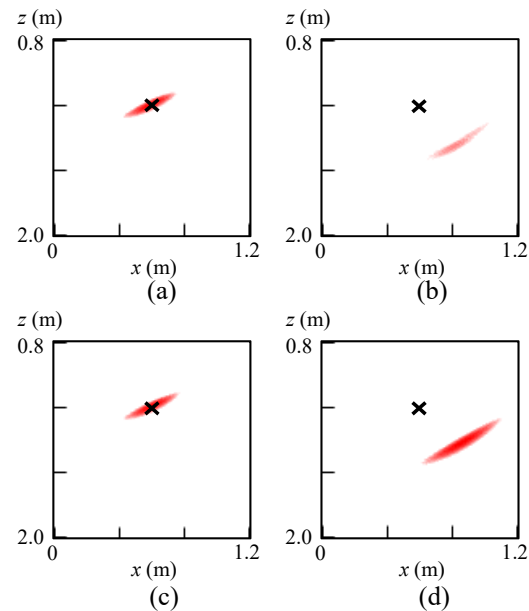


Fig. 3 Examples of calculated image: (a) cross-type $c = 190$ [m/s], (b) cross-type $c = 230$ [m/s], (c) circular-type $c = 190$ [m/s], and (d) circular-type $c = 230$ [m/s].

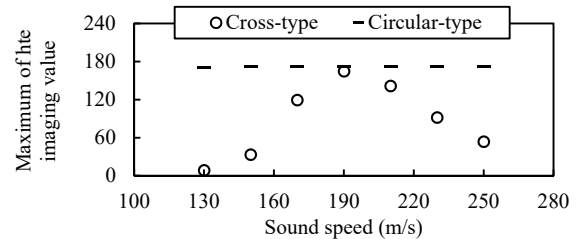


Fig. 4 Sound Speed estimation

shows the object at an incorrect position with high imaging value.

6. Conclusions

We proposed the sound speed estimation for underground imaging, and discussed the effectiveness of array arrangement on sound estimation by simulation.

By using the cross-type arrangement, the correct sound speed estimation can be expected.

Acknowledgment

This work was partly supported by a MEXT Supported Program for the Strategic Research Foundation at Private Universities (S1311004).

References

1. L. Tao, et al: Jpn. J. Appl. Phys. **38** (1999) 3148.
2. Y. Matsuo, et al: Jpn. J. Appl. Phys. **41** (2002) 3539.
3. L. Tao and S. Motooka: Jpn. J. Appl. Phys. **46** (2007) 4589.
4. R. Toh and S. Motooka: IEICE Trans. **J94-A** (2011) 870.